Iranian Journal of Medical Physics
Vol. 12, No. 1, Winter 2015, 7-13
Received: July 13, 2014; Accepted: October 28, 2014

Original Article

Calculation of Positron Distribution in the Presence of a Uniform Magnetic Field for the Improvement of Positron Emission Tomography (PET) Imaging Using GEANT4 Toolkit

Mohsen Mashayekhi[1], Ali Asghar Mowlavi[1,2]

Abstract

Introduction
Range and diffusion of positron-emitting radiopharmaceuticals are important parameters for image resolution in positron emission tomography (PET). In this study, GEANT4 toolkit was applied to study positron diffusion in soft tissues with and without a magnetic field for six commonly used isotopes in PET imaging including ^{11}C, ^{13}N, ^{15}O, ^{18}F, ^{68}Ga, and ^{82}Rb.

Materials and Methods
GEANT4 toolkit was used to simulate the transport and interactions of positrons. Calculations were performed for the soft tissue phantom (8 mm ×8 mm × 8 mm). Positrons were emitted isotropically from the center of the phantom. By the application of a magnetic field perpendicular to the path of positrons, lateral scattering of positrons could be prevented due to Lorentz force. When the positron energy was below the cut-off threshold (0.001 MeV), the simulation was terminated.

Results
The findings showed that the presence of a magnetic field increased the rate of positron annihilation. At magnetic field strengths of 3, 7, and 10 Tesla, ^{18}F with the lowest decay energy showed improvements in the ratio of full width at half maximum (FWHM) resolution to the peak of curve by 3.64%, 3.89%, and 5.96%, respectively. In addition, at magnetic field strengths of 3, 7 and 10 Tesla, ^{82}Rb with the highest decay energy showed improvements in resolution by 33%, 85%, and 99%, respectively.

Conclusion
Application of a magnetic field perpendicular to the positron diffusion plane prevented the scattering of positrons, and consequently, improved the intrinsic spatial resolution of PET imaging, caused by positron range effects.

Keywords: Positron; PET Image; Magnetic Field; GEANT4 Toolkit

1- Physics Department, Hakim Sabzevari University, Sabzevar, Iran.
2- International Centre for Theoretical Physics (ICTP), Associate and Federation Schemes, Medical Physics Field, Trieste, Italy.
*Corresponding author: Tel: +98 51 4003159; Fax: +98 51 4003170; E-mail: amolavi@ictp.it , amwolavi@hsu.ac.ir

1. Introduction

Cancer is a major public health concern, worldwide. In total, 25% of all deaths in Europe have been associated with different types of cancer. In fact, cancer is the main cause of mortality in the age range of 45-65 years [1].

The main goal in cancer treatment is to destroy tumor tissues and spare the adjacent healthy tissues [2]. Positron emission tomography (PET) is a commonly used technique for imaging tumors and malignant lesions in the body. It is clear that PET relies upon the detection of photons, resulting from the annihilation of positrons emitted by radiopharmaceuticals. There are three factors limiting the intrinsic spatial resolution of a PET system [3, 4]: 1) the diffusion range of positrons; 2) non-collinear annihilation; and 3) finite detector width.

As positron particles move through the matter, they continually lose their energy in collisions, mainly with electrons present in the absorbing material. When a positron reaches near the end of its range, it annihilates with an electron, producing two 0.511 MeV photons. Coincidence detection of these two collinear photons by PET camera is used to image cancer tumors. Due to the multiple scattering of positrons, their path in the tissue is far from a straight line and this phenomenon causes resolution reduction.

The integration of PET and magnetic resonance imaging (MRI) has attracted the researchers' attention in recent years [5-10]. By the application of a magnetic field perpendicular to the positron path, lateral scattering of positrons can be prevented due to Lorentz force. Therefore, positron annihilation points in the tumor area are increased.

Full width at half maximum (FWHM) of positron distribution curve represents the intrinsic spatial resolution of PET imaging. In this study, we initially applied GEANT4 toolkit to evaluate the ratio of FWHM to the peak of positrons' distribution. Moreover, the parameters of Derenzo's formula were obtained from the fitting processes with positron distribution curve for the isotopes [11]. Finally, the effects of the uniform magnetic field (strengths of 3, 7 and 10 Tesla) on the distribution of positron end-points were studied.

2. Materials and Methods

2.1. The effect of magnetic field on the end-point energy distribution of positrons

When positrons are located in the magnetic field, they are affected by Lorentz force:

$$\vec{F}_{Lor} = q\vec{v} \times \vec{B} \quad (1)$$

where $\vec{V}$ is the positron's velocity vector, $\vec{B}$ is the magnetic field vector, and q is the particle's charge. It is clear that Lorentz force is perpendicular to the magnetic field and the particle's velocity. Therefore, if a particle moves parallel to the field, it will not experience any force. If a positron moves at an angle to the magnetic field axis, its path will be helical. The radius of this helix is obtained by Enge's formula, which is as follows [12]:

$$R = \frac{0.334}{B}\sqrt{(2m_p c^2 E_t) + E^2{}_t} \quad (2)$$

where B is the magnetic field, $m_p c^2$ is 0.511 MeV as the positron rest mass, and E_t is the component of positron's kinetic energy perpendicular to the magnetic field in MeV scale. Thus, application of the magnetic field reduced the positrons' range which could prevent their lateral dispersion.

2.2. Geant4 toolkit and positron emitting sources

Geant4 version 4.9.6.02 is a C++ toolkit for simulating the transport and interactions of particles in the matter, facilitating a comprehensive set of physical processes over a wide range of energies [13]. This model is used in physics list contained the standard package for Electromagnetic interactions.

First, the positrons were emitted isotropically from the center of soft tissue phantom (8 mm × 8 mm × 8 mm). The positrons lost a certain amount of energy after traveling a distance; this energy was determined by differential energy loss and interaction cross-sections

inside the soft tissue [14]. The elemental composition of the soft tissue was considered to be 0.1% hydrogen, 0.11% carbon, 0.02% nitrogen, and 0.76% oxygen, respectively.

Based on pair-annihilation phenomenon, when a positron loses its kinetic energy, it can combine with an electron, and thus, two 0.511 MeV gamma rays in opposite directions are emitted. In our study, the energy, position, and velocity vectors were recorded after each step with and without the magnetic fields (strengths of 3, 7 and 10 Tesla). When the positron's energy was below 0.001 MeV (as the cut-off threshold), the simulation process was terminated. We followed 2×10^{6} particles in each simulation.

The positron energy spectra of six commonly used isotopes (^{11}C, ^{13}N, ^{15}O, ^{18}F, ^{68}Ga and ^{82}Rb) are shown in figure 1 [15].

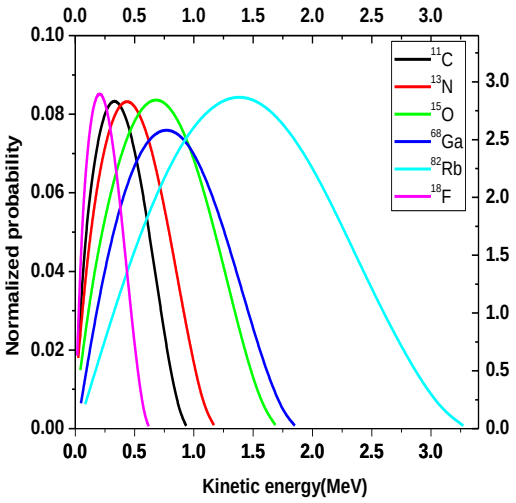

Figure 1. Distribution of positron energy spectra for six commonly used isotopes in PET imaging

3. Results

PET relies upon the detection of photons resulting from the annihilation of positrons emitted by radiopharmaceuticals. The combination of images obtained from PET and MRI has begun to greatly enhance the study of many physiological processes. In this study, a strong static homogeneous magnetic field was used to increase PET resolution by reducing the effects of positron range. As the results indicated, the resolution of PET images could be improved due to the effects of the magnetic field.

Distribution of positron end-points for the isotopes in the absence of the magnetic field is shown in Figure 2. By applying the magnetic field along the Z direction, positron diffusion was confined in the X-Y plane. The simulation results for magnetic field strengths of 3, 7 and 10 Tesla are presented in Figure 3.

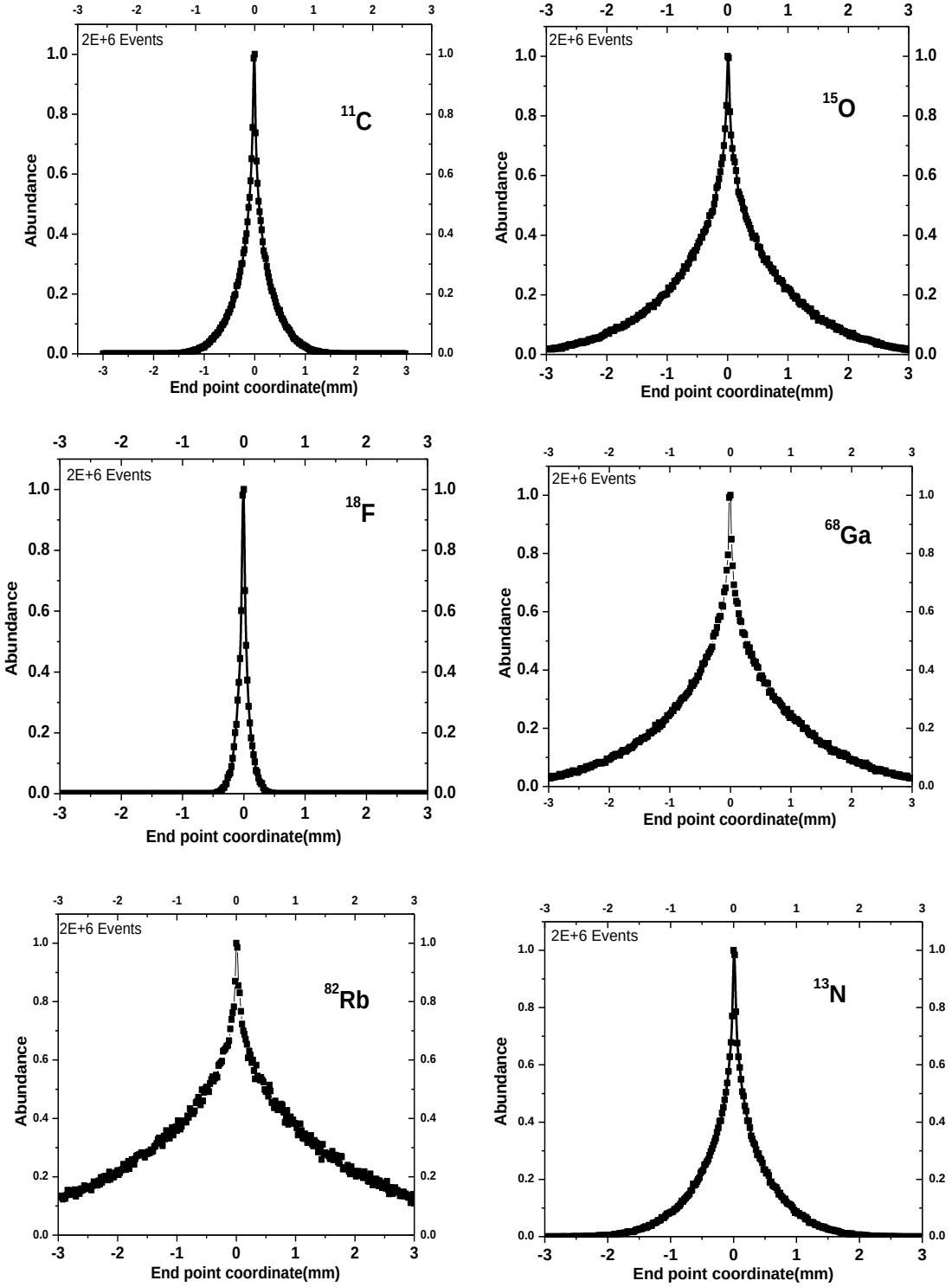

Figure 2: Distribution of positron end-points for six radioisotopes in the absence of the magnetic field

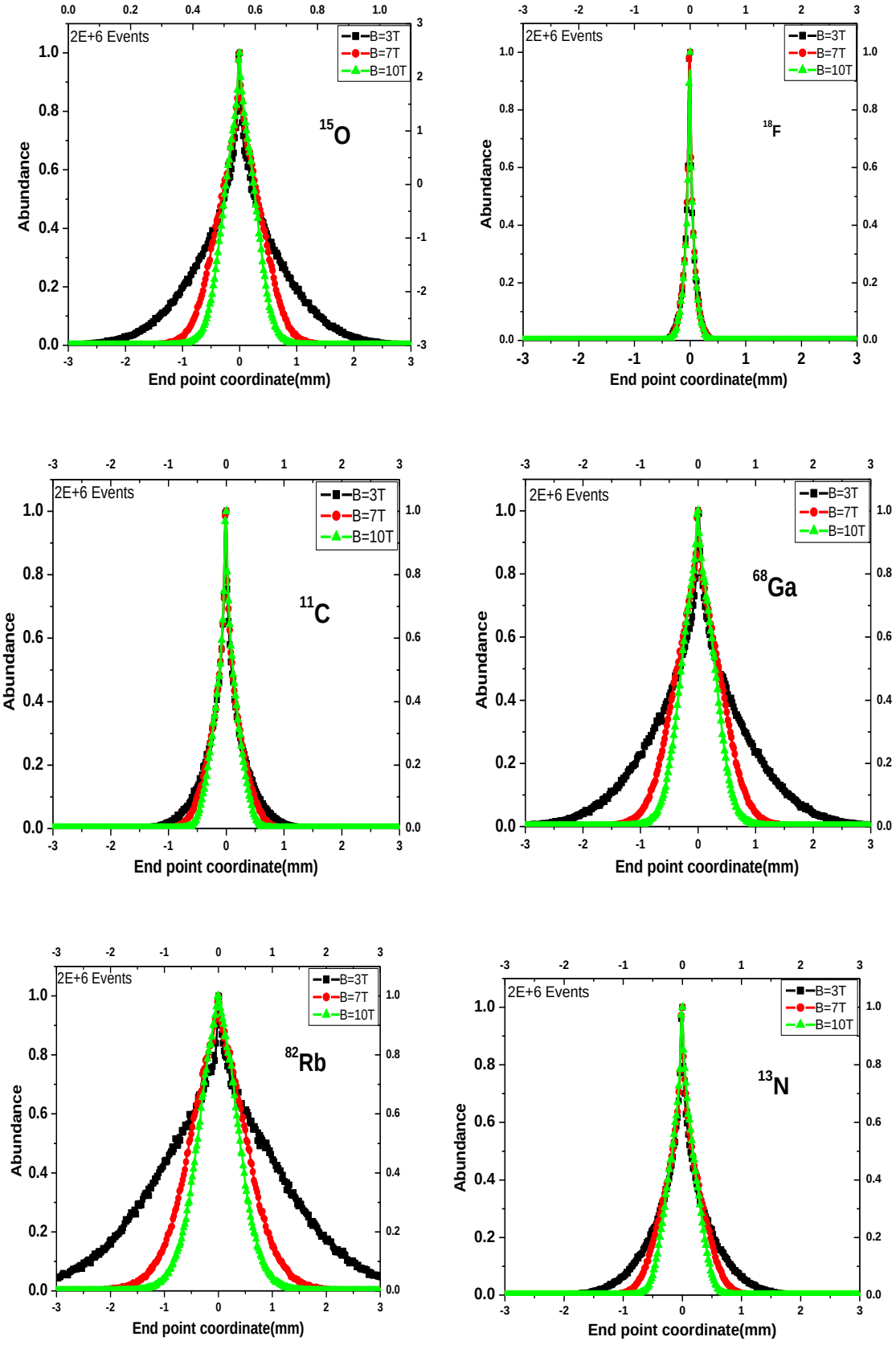

Figure 3: Distribution of positron end-points for six radioisotopes in the presence of the magnetic field

4. Discussion

In figures 2 and 3, horizontal and vertical axes represent the distance from the origin, ranging from −3 to 3 mm and the abundance of annihilated positrons, respectively. In order to calculate and analyze the results in the presence and absence of magnetic fields, the fitted parameters and the ratio of FWHM to the peak of positron distribution were obtained, based on Derenzo's formula [11]:

$$p(x) = k_3 e^{-k_1 x} + (1-k_3) e^{-k_2 x} \quad (x \geq 0) \qquad (3)$$

The results showed that magnetic fields have a significant effect over high-energy positron spectra. At magnetic field strengths of 3, 7, and 10 Tesla, ^{18}F with the lowest decay energy showed improvements in the ratio of FWHM resolution to the peak of curve by 3.64%, 3.89%, and 5.96%, respectively. In addition, at magnetic field strengths of 3, 7 and 10 Tesla, ^{82}Rb with the highest decay energy showed improvements in resolution by 33%, 85%, and 99%, respectively.

The results regarding the ratio of FWHM to the peak of curve in the absence of the magnetic field and the fitted parameters based on formula (3) are listed in Table 1. The results related to the presence of the magnetic field are illustrated in Table 2. It should be noted that the maximum error of calculation was approximately 7%.

Table 1: Fitted parameters based on formula (3), the maximum energy of emitted positrons, and the ratio of FWHM to the peak of positrons' distribution curve, without the magnetic field; H is the peak of positron distribution.

Positron emitter	$E_{\max}(MeV)$	k_3	$k_1(mm^{-1})$	$k_2(mm^{-1})$	$\frac{FWHM(0T)}{H(0T)}$
^{18}F	0.61	0.32	50	10.75	8.22E-5
^{11}C	0.93	0.35	4.66	3.22	1.10E-4
^{13}N	1.16	0.41	16.94	2.04	1.69E-4
^{15}O	1.68	0.38	14.70	1.11	3.60E-4
^{68}Ga	1.85	0.63	0.96	19.12	4.32E-4
^{82}Rb	3.27	0.65	0.55	10.71	1.3E-3

Table 2: The simulation results for the ratio of FWHM to the peak of positrons' distribution curve in the presence and absence of the magnetic field (strengths of 3, 7 and 10 Tesla)

Positron emitter	$\frac{FWHM(0T)}{H(0T)}$	$\frac{FWHM(3T)}{H(3T)}$	$\frac{FWHM(7T)}{H(7T)}$	$\frac{FWHM(10T)}{H(10T)}$
^{18}F	8.22E-5	7.92E-5	7.90E-5	7.73E-5
^{11}C	1.10E-4	1.01E-4	5.71E-5	5.67E-5
^{13}N	1.69E-4	1.45E-4	8.81E-5	5.1E-5
^{15}O	3.60E-4	2.87E-4	9.99E-5	5.19E-5
^{68}Ga	4.32E-4	3.28E-4	1.05E-4	5.39E-5
^{82}Rb	1.3E-3	0.87E-3	0.19E-3	9.73E-5

5. Conclusion

Both PET and MRI are common diagnostic imaging modalities in pharmaceutical research. Combination of these two imaging procedures could improve the in-plane resolution of PET images, considering the effects of magnetic field on positron transport and the annihilation process. In general, inside the magnetic fields, a positron is subjected to the Lorenz force and its trajectory changes from a straight line to a spiral curve. The radius of such a spiral curve is proportional to the positron energy.

As the results indicated (Figure 3), application of a magnetic field perpendicular to the positrons' diffusion plane prevented their scattering and increased the number of positron end-points around the origin. Overall, as the decay energy of a positron-emitting radioinuclide is increased, the positrons can diffuse longer distances on average.

The distribution of positron end-points was compressed in the magnetic field. When the

magnetic field was applied along the Z direction, the compression only occurred orthogonal to but not along the Z direction. This implies that only the transaxial resolution of the PET system is improved in a concentric PET/MRI scanner.

For ^{18}F and ^{82}Rb, the image resolution improved by 3.64%-5.96% and 33%-99% in the presence of varying magnetic field strengths (3 to 10 Tesla), respectively. Thus, a high-intensity magnetic field can effectively increase the resolution of PET imaging. Thisphenomenon is important in combined PET/MRI systems.

Acknowledgements

Authors would like to thanks Hakim Sabzevari University for the supports.

References

1. Niederlaender E. Causes of death in the EU. Statistics in focus: population and social conditions. 2006;KS-NK-06-010-EN-N.
2. Yock TI, Tarbell NJ. Technology insight: Proton beam radiotherapy for treatment in pediatric brain tumors. Nat Clin Pract Oncol. 2004 Dec;1(2):97-103
3. Levin CS, Hoffman EJ. Calculation of positron range and its effect on the fundamental limit of positron emission tomography system spatial resolution. Phys Med Biol. 1999 Mar;44(3):781-99.
4. Catana C, Procissi D, Wu Y, Judenhofer MS, Qi J, Pichler BJ, et al. Simultaneous in vivo positron emission tomography and magnetic resonance imaging. Proc Natl Acad Sci USA. 2008 Mar;105(10):3705-10.
5. Marsden PK et al. Simultaneous PET and NMR. Br J Radiol. 2002;75 53–9.
6. Zaidi H, Montandon ML, Slosman DO. Magnetic resonance imaging-guided attenuation and scatter corrections in three-dimensional brain positron emission tomography. Med Phys. 2003 May;30(5):937-48.
7. Takasawa M, Jones PS, Guadagno JV, Christensen S, Fryer TD, Harding S, et al. How reliable is perfusion MR in acute stroke? Validation and determination of the penumbra threshold against quantitative PET. Stroke. 2008;39(3):870-7.
8. Cherry SR. Multimodality in vivo imaging systems: twice the power or double the trouble? Annu Rev Biomed Eng. 2006;8:35-62.
9. Catana C, Procissi D, Wu Y, Judenhofer MS, Qi J, Pichler BJ, et al. Simultaneous in vivo positron emission tomography and magnetic resonance imaging. Proceedings of the National Academy of Sciences. 2008;105(10):3705-10.
10. Pichler BJ, Kolb A, Nagele T, Schlemmer HP. PET/MRI: paving the way for the next generation of clinical multimodality imaging applications. J Nucl Med. 2010;51(3):333-6.
11. Derenzo SE. Precision measurement of annihilation point spread distributions for medically important positronemitters Positron Annihilation. Sendai, The Japan Institute of Metals, 1979.
12. Enge H. Introduction to Nuclear Physics, 2nd ed. Reading, MA: Addision-Wesley, 1966.
13. Agostinelli S, Allison J, Amako Ka, Apostolakis J, Araujo H, Arce P, et al. GEANT4—a simulation toolkit. Nuclear Instruments and Methods in Physics Research Section A: Accelerators, Spectrometers, Detectors and Associated Equipment. 2003;506(3):250-303.
14. Geant4 Material Database, 2015. Available from: http://geant4.web.cern.ch/geant4/G4UsersDocuments/UsersGuides /ForApplicationDeveloper/html/Detector/materialNames.html
15. RADAR - The Decay Data, 2002. Available from: http://www.doseinfo-radar.com/RADARDecay.html